Crystal engineering of two-dimensional polar layer structures: hydrogen bond networks in some *N-meta*-phenylpyrimidinones

Sumod George,[a] Ashwini Nangia,*[a] Muriel Bagieu-Beucher,[b] René Masse*[b] and Jean-François Nicoud[c]

[a] *School of Chemistry, University of Hyderabad, Hyderabad 500 046, India. E-mail: ansc@uohyd.ernet.in*
[b] *Laboratoire de Cristallographie (associé à l'Université Joseph Fourier), CNRS, B.P. 166, 38042, Grenoble cedex, France. E-mail: masse@labs.polycnrs-gre.fr*
[c] *Groupe de Matériaux Organiques, Institut de Physique et Chimie des Matériaux de Strasbourg (CNRS UMR 7504), Université Louis Pasteur, 23 rue du Loess, 67037 ż, Strasbourg cedex, France*

Received (in Montpellier, France) 19th July 2002, Accepted 23rd November 2002
First published as an Advance Article on the web 28th January 2003

In a recent paper (*New J. Chem.*, 2001, **25**, 1520), we have analysed crystal structures of some *N*-aryl pyrimidinones. Based on the occurrence of two-dimensional layers in six out of nine crystals, we proposed that self-assembly in these structures might be analysed in terms of the stacking of 2D hydrogen-bonded layers. We show herein that *meta*-substituted phenyl pyrimidinones (Br, I, F, NO_2, Me, OMe) have an overwhelming preference for the 2D polar arrangement, namely the parallel alignment of 1D chains within a layer. The molecules are arranged in chains mediated by C–H···O hydrogen bonds and such motifs are connected *via* C–H···O and C–H···halogen interactions in the lateral direction. A notable feature in these structures is that chains of dipolar molecules align in a parallel fashion to produce polar layers. The preference for 2D polarity is explained by the shape of the aryl pyrimidinone molecule and the geometry of interactions between hydrogen bonding functional groups (C–H donors, O/halogen acceptors). However, the polar layers stack in an anti-parallel manner and the crystal structures are centrosymmetric. The task of controlling parallel stacking of polar domains in the 3D crystal is a continuing challenge in our studies.

Introduction

The physical and chemical properties of a crystal are governed not only by the nature of the constituent molecules but also by the nature of hydrogen bonds and intermolecular interactions in the condensed phase.[1] Crystal engineering,[2] the design of organic solid-state structures with hydrogen bonds and intermolecular interactions, is intimately linked with the principles of self-assembly and molecular recognition, the paradigm in supramolecular chemistry.[3] The implications of crystal engineering today go far beyond the study of intermolecular interactions and the design of crystal structures with aesthetic appeal and utilitarian considerations into the realms of pharmaceutical development (*e.g.*, pharmacophore mapping, drug-receptor models) and synthetic chemistry (*e.g.*, stereocontrolled topochemical reactions, tailor-made catalysts).[4] Rational approaches to crystal design are guided by a combination of factors: (1) a proper understanding of the strength and directionality of hydrogen bonds (O–H···O, N–H···O, C–H···O) and intermolecular interactions;[5] (2) the crystallographic data on over 250 000 organic and organometallic structures archived in the Cambridge Structural Database[6] and (3) supramolecular synthons,[7] or structural units, that encapsulate the recognition information during crystallisation.

Crystallisation of achiral molecules in non-centrosymmetric space groups is a current challenge in crystal engineering.[8] Despite the potential of chiral or polar hydrogen-bonded solids in materials science (*e.g.*, ferroelectric, nonlinear optics), there are no general solutions so far for inducing self-assembly of achiral molecules into space groups that lack an inversion centre.[9] † In the context of rational approaches to engineering polar materials, Hollingsworth and Hulliger have shown that channel-type inclusion compounds have considerable promise for the parallel alignment of dipolar molecules.[10] Two-dimensional host frameworks have been utilised to produce polar crystallographic symmetries through crystal engineering of the flexible hydrogen-bonded sheets with banana-shaped pillars.[11] Lin's group has shown that diamondoid networks couple high thermal stability with high SHG activity.[8b,12] Our approach to this problem is modular: the 3D polar structure is dissected into 2D polar layers that must stack in a parallel fashion. This simplifies the difficult task of steering the parallel alignment of dipoles to the third dimension. Such a modular build-up of 3D architectures (= 2D + 1D) from tailor-made molecules has been successfully implemented in hydrogen-bonded solids, for example, lamellar clay-type intercalates with guanidinium cations and sulfonate anion organic pillars.[11] However, single component crystals and organic salts offer certain advantages compared to inclusion adducts for materials applications, such as thermal and mechanical stability and ease of crystal growth.

We have reported X-ray crystal structures of *N*-arylpyrimidinone, **1** (aryl = phenyl, tolyl, halophenyl), and their HCl and

† Polar arrangement of chromophores can be realised in enantiomorphous or non-enantiomorphous non-centrosymmetric point groups. The distinction between polar, enantiomorphous, non-centrosymmetric for third rank tensor property NLO is very important but in this paper we are only concerned with the arrangement of polar motifs of chromophores capable of forming non-centrosymmetric structures.

 DOI: 10.1039/b207090a

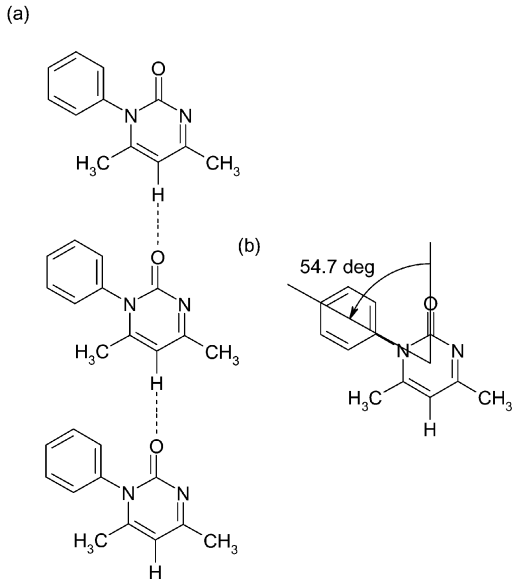

Fig. 1 (a) C–H···O hydrogen-bonded chain of phenyl pyrimidinone molecules **1**. (b) The tilt of the charge transfer axis with respect to the polar axis in **1**. The ideal angle is 54.7°; the observed values in **1** are 57–60°.

HNO_3 salts.[13] Our initial experiments with nine derivatives of phenyl pyrimidinone (**1**H, **1***p*-Me, **1***p*-Cl, **1***p*-Ph, **1**H·HCl, **1***p*-Me·HCl, **1***p*-Cl·HCl, **1***p*-Me·HNO_3 and **1***p*-Cl·HNO_3) gave the following results. (1) The recurrence of a C–H···O hydrogen bond chain involving the activated sp^2 C–H donor and carbonyl acceptor in these crystals (Fig. 1). (2) The occurrence of a mirror plane *m* in eight out of nine structures. (3) Six of the nine structures have a 2D polar layer arrangement, that is, the dipoles are aligned parallel within a hydrogen-bonded layer. (4) The charge transfer axis of the chromophore is tilted with respect to the main symmetry operator in point groups 2 or *m* at an angle of *ca.* 57° (ideal value is 54.74°), a requirement in NLO materials (Fig. 1).[14] We have addressed points (1) and (2) in previous papers,[13] and now take up the engineering of 2D polar layers in crystals. The X-ray crystal structures of *meta*-phenyl pyrimidinones (**1**) and pyrimidinones (**2**) are discussed in this paper. A model is proposed to explain the recurrence of the 2D polar layer assembly in these structures. It should be mentioned that the polar layers in **1** and **2** stack in an anti-parallel fashion and the crystal structures are centrosymmetric with no immediate materials application. Nevertheless, we have continued this study because the factors that control parallel *vs.* anti-parallel alignment of domains are not properly understood.[15] This paper deals with the parallel alignment of dipolar molecules **1** within a hydrogen-bonded layer. Two-dimensional layered structures have been assembled using strong O–H···O and N–H···O hydrogen bond networks with urea-based building blocks.[16] We show herein that pyrimidinone **1** results in 2D layered motifs stabilised by weak C–H···O and C–H···halogen interactions.

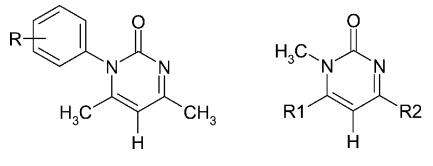

1

R = H, *p*-Me, *p*-Cl, *p*-Ph, *m*-Br, *m*-I, *m*-NO_2, *m*-Me, *m*-OMe, *m*-F

2

a: R1 = Me, R2 = Ph
b: R1 = Ph, R2 = Me

Some current approaches for inducing crystallisation of achiral molecules in non-centrosymmetric space groups include molecular octupoles,[17] donor-acceptor complexes,[18] interpenetrated networks,[8b,12,19] channel inclusion adducts,[10,20] and polar lamellar solids.[11] However, many of these materials display modest SHG activity, in part because the dipolar molecules are constrained in an inactive host lattice.

Experimental

Synthesis

The appropriate *N*-aryl urea[21] was condensed with acetyl acetone to afford the *N*-arylpyrimidinone **1**. Yields are unoptimised and reported for purified products isolated after column chromatography. NMR spectra were recorded on a Bruker 200 MHz spectrometer in $CDCl_3$ solvent. Peaks are reported in δ and the *J* coupling in Hz, followed by proton integration. IR spectra were recorded as KBr wafers, peaks are reported in cm^{-1}.

1,2-Dihydro-*N*-*meta*-bromophenyl-4,6-dimethylpyrimidin-2-one (1*m*-Br). Acetyl acetone (900 mg, 0.92 ml, 9 mmol) and *N*-*meta*-bromophenyl urea (500 mg, 3 mmol) were taken up in 10 mL of EtOH and 1.8 mL of conc. HCl was added. The reaction mixture was refluxed for 4 h, then cooled in ice, and the precipitated solid was filtered and washed with cold EtOH to obtain the hydrochloride salt. The salt was dissolved in 10 mL of water and neutralised with NaOH solution (0.7 g in 5 mL of water) at 0 °C. Extraction of the aqueous layer with chloroform and evaporation of the solvent afforded the product (17% yield), which was crystallised from an ethyl acetate–hexane mixture. M.p. 179–183 °C. ^{1}H NMR: 7.65 (d, $J = 8$, 1H), 7.40 (s, 1H), 7.34 (t, $J = 8$, 1H), 7.18 (d, $J = 8$, 1H), 6.19 (s, 1H), 2.41 (s, 3H), 2.05 (s, 3H). IR: 3053, 1653, 1527.

1,2-Dihydro-*N*-*meta*-iodophenyl-4,6-dimethylpyrimidin-2-one (1*m*-I). Crystallised from an ethyl acetate–hexane mixture, m.p. 168–170 °C, yield 26%. ^{1}H NMR: 7.85 (d, $J = 8$, 1H), 7.65 (s, 1H), 7.29 (d, $J = 8$, 1H), 7.25 (t, $J = 8$, 1H), 6.19 (s, 1H), 2.43 (s, 3H), 2.05 (s, 3H). IR: 3232, 1643, 1531.

1,2-Dihydro-*N*-*meta*-nitrophenyl-4,6-dimethylpyrimidin-2-one (1*m*-NO_2). Crystallised from methanol, m.p. 236–240 °C, yield 34%. ^{1}H NMR: 8.37 (d, $J = 8$, 1H), 8.15 (s, 1H), 7.75 (t, $J = 8$, 1H), 7.65 (d, $J = 8$, 1H), 6.25 (s, 1H), 2.42 (s, 3H), 2.09 (s, 3H). IR: 3082, 1649, 1525, 1346.

1,2-Dihydro-*N*-*meta*-tolyl-4,6-dimethylpyrimidin-2-one (1*m*-Me). Crystallised from a benzene–ethyl acetate mixture, m.p. 186–189 °C, yield 25%. ^{1}H NMR: 7.41 (t, $J = 8$, 1H), 7.30 (d, $J = 8$, 1H), 7.05 (d, $J = 8$, 1H), 7.10 (s, 1H), 6.20 (s, 1H), 2.45 (s, 6H), 2.05 (s, 3H). IR: 3049, 1651, 1531.

1,2-Dihydro-*N*-*meta*-anisyl-4,6-dimethylpyrimidin-2-one (1*m*-OMe). Crystallised from a benzene–ethyl acetate mixture, m.p. 137–141 °C, yield 23%. ^{1}H NMR: 7.40 (t, $J = 8$, 1H), 7.05 (d, $J = 8$, 1H), 6.80 (d, $J = 8$, 1H), 6.79 (s, 1H), 6.18 (s, 1H), 3.85 (s, 3H), 2.40 (s, 3H), 2.05 (s, 3H). IR: 3053, 1668, 1535.

1,2-Dihydro-*N*-*meta*-flourophenyl-4,6-dimethylpyrimidin-2-one (1*m*-F). Crystallised from a benzene–ethyl acetate mixture, m.p. 175–183 °C, yield 26%. ^{1}H NMR: 7.50 (dd, $J = 8,7$, 1H), 7.20 (dd, $J = 8,7$, 1H), 6.97 (d, $J = 8$, 1H), 6.91 (d, $J = 8$, 1H), 6.19 (s, 1H), 2.45 (s, 3H), 2.01 (s, 3H). IR: 3065, 1651, 1533.

1,2-Dihydro-*N*-methyl-4-methyl-6-phenylpyrimidin-2-one and 1,2-dihydro-*N*-methyl-4-phenyl-6-methylpyrimidin-2-one (2a and 2b). Benzoyl acetone (1.42 g, 9 mmol) and *N*-methyl urea (500 mg, 7 mmol) were taken up in 10 mL of EtOH and

1.65 mL of conc. HCl was added. The reaction mixture was refluxed for 4 h, then cooled in ice, and the precipitated solid was filtered and washed with cold EtOH to obtain the hydrochloride salt. The salt was dissolved in 10 mL of water and neutralised with NaOH solution (0.7 g in 5 mL of water) at 0 °C. Extraction of the aqueous layer with chloroform and evaporation of the solvent afforded the product as a mixture of isomers in 22% yield. Isomers **2a** and **2b** were separated by column chromatography using neutral silica with 80:20 ethyl acetate–hexane eluent. The tentative assignment of regioisomers **2a** and **2b** based on NMR and IR spectra is confirmed by single crystal X-ray diffraction.

2a. Crystallised from ethyl acetate–hexane, m.p. 169–171 °C. ^{1}H NMR: 8.11 (d, $J = 8$, 2H), 7.40–7.50 (m, 3H), 6.71 (s, 1H), 3.62 (s, 3H), 2.44 (s, 3H). IR: 3057, 1630, 1579, 1535, 1494, 1354.

2b. Crystallised from ethyl acetate–hexane, m.p. 186–188 °C. ^{1}H NMR: 7.40–7.60 (m, 3H), 7.30 (d, $J = 8$, 2H), 6.15 (s, 1H), 3.39 (s, 3H), 2.35 (s, 3H). IR: 1651, 1539, 1489, 1072, 1026, 958.

Crystallography

Single crystal X-ray data was collected on a Nonius-CAD4 diffractometer with Mo*K*α radiation (λ 0.7107 Å) and on a Nonius-CCD Kappa diffractometer working with Ag*K*α radiation (λ 0.5608 Å) from 180 exposures with Δφ scans, $\Delta\phi = 1°$. $\theta_{max} = 35.2°$ (CAD4) and 21.5° (or 27.9° exceptionally) on the CCD. Absorption correction was applied for the Br and I atoms. Hydrogen atoms were refined in such a way that the ratio of reflections to parameters for each crystal structure is favourable, that is, about 10. Structures were solved using direct methods with SIR92 program.[22a] Full-matrix least-squares refinement were performed on *F* using the teXsan software.[22b] Scattering factors for neutral atoms and f', $\Delta f'$, f'', $\Delta f''$ were taken from the *International Tables for X-ray Crystallography*.[22c] Details of crystal data collection, structure solution and refinement are listed in Table 1 and metrics of some important hydrogen bonds are summarised in Table 2. Crystal packing diagrams were drawn using PLATON.[22d]

CCDC reference numbers 200184–91. See http://www.rsc.org/suppdata/nj/b2/b207090a/ for crystallographic files in CIF or other electronic format.

Results and discussion

Phenylpyrimidinone **1** was synthesised as described previously.[13] Pyrimidinone **2** was synthesised by the condensation of *N*-methylurea with benzoyl acetone and separation of isomers **2a** and **2b** by column chromatography. Crystallisation of **1** and **2** from different solvents (*e.g.*, ethanol, benzene, ethyl acetate, hexane, and their mixtures) afforded diffraction quality crystals (Table 1). The arrangement of molecules in the eight crystal structures discussed is mediated by weak hydrogen bonds[5] (C–H···O, C–H···halogen) and van der Waals interactions. The structures are analysed in this sequence: **1***m*-Br, **1***m*-I, **1***m*-NO_2, **1***m*-Me, **1***m*-OMe, **1***m*-F, **2a** and **2b**.

1,2-Dihydro-*N*-*meta*-X-phenyl-4,6-dimethylpyrimidin-2-one (X = Br, I, NO_2)

In the crystal structure of **1***m*-Br (space group $P\bar{1}$), translation-related molecules are connected by a chain of C–H···O hydrogen bonds [*d*, θ: 2.47(4) Å, 154(3)°] along the *a* axis. These chains are connected by a C–H···Br interaction[23] [3.12(5) Å, 121(3)°] in the lateral direction to produce a rectangular grid network in the (0 1 $\bar{1}$) plane [Fig. 2(a)]. It may be noted that the carbonyl groups of **1***m*-Br point in the same direction within a layer, referred to as 2D polarity in this discussion. In effect, linear chains of C–H···O and C–H···Br interactions traverse to produce a polar sheet structure. The interlayer region has a profusion of C–H···O/C–H···Br interactions (Table 2) and an overall hydrophobic fit. The crystal structure is centrosymmetric; adjacent layers are inversion-related [Fig. 2(b)].

The *N*-phenyl ring in **1***m*-Br is tilted with respect to the pyrimidinone ring at an angle of 74.8(5)°. In symmetrical phenyl derivatives of **1** (*e.g.*, Ph, *para*-tolyl, *para*-chlorophenyl), the aryl and heterocyclic ring are exactly perpendicular to each other such that the pyrimidinone ring lies in the mirror plane and the *m* plane bisects the phenyl ring. We have explained the orthogonal orientation of aryl and pyrimidinone rings in symmetrical derivatives of **1** by calculating the energy of the isolated molecule as a function of the interplanar dihedral angle (τ/°) in the RHF 3-21G* basis set.[13b] The energy *vs.* dihedral angle curve, with a minimum at $\tau = 90°$, is very shallow in the region $80° < \tau < 100°$. A slight deviation from the perpendicular conformation is tolerated if such a tilt results in favourable interactions elsewhere in the crystal. The weak

Table 1 Crystal data for compounds in this study

Compound	**1***meta*-Br	**1***meta*-I	**1***meta*-NO_2	**1***meta*-Me	**1***meta*-OMe	**1***meta*-F	4-Me,6-Ph (**2a**)	4-Ph,6-Me (**2b**)
Chemical formula	$C_{12}H_{11}BrN_2O$	$C_{12}H_{11}IN_2O$	$C_{12}H_{11}N_3O_3$	$C_{13}H_{14}N_2O$	$C_{13}H_{14}N_2O_2$	$C_{12}H_{10}FN_2O$	$C_{12}H_{12}N_2O$	$C_{12}H_{12}N_2O$
Formula weight	279	326	245	214	230.27	217.22	200.24	200.24
T/K	296.2	296.2	296.2	296.2	296.2	296.2	273.2	296.2
Crystal system	Triclinic	Triclinic	Triclinic	Monoclinic	Monoclinic	Orthorhombic	Orthorhombic	Monoclinic
Space group	$P\bar{1}$	$P\bar{1}$	$P\bar{1}$	$P2_1/n$	$C2/c$	*Pnma*	*Pbca*	$C2/c$
a/Å	7.1084(6)	7.531(1)	7.126(6)	7.1729(5)	21.324(4)	7.0475(10)	10.1248(7)	18.468(3)
b/Å	7.4863(6)	12.236(2)	7.635(1)	14.506(2)	7.2771(9)	7.438(3)	17.625(2)	7.214(2)
c/Å	11.923(1)	7.154(1)	11.337(2)	11.384(1)	16.929(7)	20.763(4)	11.924(1)	15.603(3)
α/deg	99.788(4)	106.27(1)	102.33(1)	90	90	90	90	90
β/deg	107.055(3)	100.1(9)	103.28(5)	106.972(6)	111.81(3)	90	90	91.87(2)
γ/deg	98.477(4)	74.90(1)	96.74(5)	90	90	90	90	90
U/Å^3	584.50(9)	607.2(7)	577.4(5)	1132.9(2)	2439.0(11)	1088.4(4)	2127.9(3)	2077.7(7)
Z	2	2	2	4	8	4	8	8
μ/mm^{-1}	1.877 (AgKα)	1.392 (AgKα)	0.104 (MoKα)	0.052 (AgKα)	0.086 (MoKα)	0.098 (MoKα)	0.052 (AgKα)	0.084 (MoKα)
N_{total}	6418	5982	5276	2693	3249	2148	4510	6672
N_{indep}	2647	2756	5071	2693	3148	1164	2756	6454
N_{used} ($I > x\sigma$)	1717 ($x = 2$)	1966 ($x = 3$)	984 ($x = 3$)	1355 ($x = 2.5$)	1437 ($x = 1$)	707 ($x = 0.5$)	1504 ($x = 2$)	1057 ($x = 3$)
R_{int}	0.06	0.05	0.041	0.00	0.02	0.052	0.036	0.05
R	0.05	0.04	0.057	0.07	0.06	0.087	0.064	0.049
R_w	0.058	0.054	0.056	0.066	0.055	0.071	0.053	0.061

Table 2 Hydrogen bond metrics in crystal structures

Compound	Hydrogen bond[a]	d/Å (H···A)	D/Å (X···A)	θ/deg ∠X–H···A
1*m*-Br	C3–H1···O1(i)	2.47(4)	3.230(5)	154(3)
	C6–H7···Br1(ii)	3.12(5)	3.723(5)	121(3)
	C12–H11···O1(iii)	2.67(4)	3.472(7)	167(4)
	C8–H8···O1(iv)	2.87(4)	3.477(6)	135(3)
	C6–H7···Br1(v)	3.28(5)	3.993(6)	131(3)
1*m*-I	C3–H1···O(i)	2.43(5)	3.267(7)	154(4)
	C6–H6···I(ii)	3.01	3.882(9)	154
	C5–H4···O(iii)	2.58(6)	3.459(7)	154(4)
	C12–H11···O(iv)	2.52(6)	3.41(1)	165(5)
	C8–H8···O(v)	2.79(6)	3.43(1)	124(4)
1*m*-NO_2	C3–H1···O1(i)	2.20	3.222(6)	156
	C6–H6···O3(ii)	2.55	3.538(6)	152
	C5–H4···O1(iii)	2.60	3.511(6)	142
	C6–H5···N3(iv)	2.70	3.730(8)	159
	C6–H5···O3(v)	2.61	3.677(8)	172
	C8–H8···O1(vi)	2.56	3.347(6)	129
	C12–H11···O1(vii)	2.39	3.423(6)	158
1*m*-Me	C3–H1···O1(i)	2.40	3.272(3)	156
	C5–H2···O1(ii)	2.81	3.655(3)	144
	C12–H11···N2(iii)	2.69	3.560(4)	140
	C8–H8···O1(iv)	2.98	3.900(4)	170
	C11–H10···O1(v)	2.90	3.581(5)	123
1*m*-OMe	C3–H1···O1(i)	2.45	3.366(3)	161
	C8–H3···O2(ii)	2.70	3.455(4)	137
	C6–H2···N2(iii)	2.46	3.391(4)	165
	C10–H5···O1(iv)	2.61	3.267(4)	126
1*m*-F	C3–H1···O1(i)	2.30	3.166(6)	154
	C6–H2···O1(ii)	2.66	3.536(5)	151
	C9–H5···F1(iii)	2.59	3.194(7)	125
4-Me,6-Ph (**2a**)	C3–H10···O1(i)	2.50(2)	3.409(4)	168(1)
	C12–H15···O1(ii)	2.48(3)	3.42(1)	164(1)
	C5–H3···N2(iii)	2.75(3)	3.691(2)	174(1)
	C6–H4···O1(iv)	2.51	3.392(3)	154
	C6–H9···O1(v)	2.57	3.392(3)	135
	C5–H2···O1(vi)	2.53(3)	3.512(9)	161(1)
4-Ph,6-Me (**2b**)	C3–H1···O1(i)	2.38	3.368(4)	149
	C8–H8···N1(ii)	2.75	3.648(4)	156
	C6–H6···O1(iii)	2.74	3.655(5)	158

[a] For illustration of interactions (i), (ii), (iii), *etc.*, see the figures.

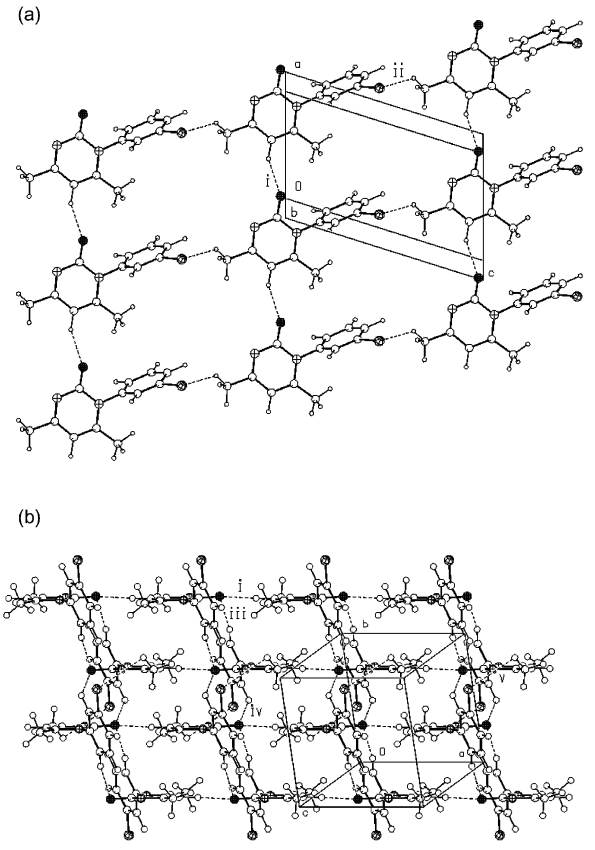

Fig. 2 Crystal structure of **1***m*-Br. (a) C–H···O hydrogen-bonded 1D chain (interaction i) and C–H···Br interaction in the lateral direction (interaction ii). Note the parallel alignment of molecules in the 2D layer. (b) Centrosymmetric arrangement of adjacent layers mediated by interactions iii, iv, v and an overall hydrophobic fit. See Table 2 for metrics of interactions in this and subsequent figures.

C–H···Br interaction in the (0 1 $\bar{1}$) direction ([Fig. 2(a); Table 2, interaction ii] is optimised as a result of the slight tilt of the phenyl ring in **1***m*-Br. In the unsymmetrical **1***m*-Br derivative, both the molecular and the crystal symmetry are lower (space group $P\bar{1}$) compared to **1***p*-Cl, **1***p*-Cl·HCl and **1***p*-Cl·HNO_3 (*Pnma*, $P2_1/m$ and *Pnma*). Thus, the *meta* derivatives crystallise in the triclinic system while the symmetrical *para* analogues crystallise in monoclinic and orthorhombic systems with a mirror plane.

Crystal structures of **1***m*-I and **1***m*-NO_2 are isostructural with **1***m*-Br, having the same space group but different cell axes and angles (Table 1). These crystal structures exhibit similar C–H···O and C–H···halogen interaction networks in the (1 1 0) and (0 1 $\bar{1}$) planes [Fig. 3(a) and 3(b)]. Thus, the 2D polar layer arrangement is observed in both these structures. However, adjacent layers are inversion-related, similar to **1***m*-Br. The (O)C–N–C–C(Ph) torsion angle (τ) is 74.0(11)° and 78.0(4)° in **1***m*-I and **1***m*-NO_2. The identical networks of lateral C–H···halogen and C–H···O(nitro) interactions highlights the importance of weak hydrogen bonds in controlling the self-assembly in these crystal structures. The calculated volume of Br, I and NO_2 groups is similar (26, 32, 29 $Å^3$),[24] and so is the arrangement of molecules in the crystal. This also testifies to the robustness of the recurring C–H···O hydrogen-bonded chain synthon (Figs. 1–3) in steering the arrangement of molecules. While the individual C–H···O interactions are weak (2–3 kcal mol^{-1}), the chain synthon constructed with these weak hydrogen bonds is strong enough to sustain self-assembly in a number of structures.

1,2-Dihydro-*N*-*meta*-X-phenyl-4,6-dimethylpyrimidin-2-one (X = Me, OMe)

The structure of **1***m*-Me (space group $P2_1/n$) contains the C–H···O hydrogen-bonded chain along the *a* axis, further stabilised by a (Me)C–H···O interaction (2.40 Å, 156°; 2.81 Å, 144°;) as shown in Fig. 4. The tolyl ring in **1***m*-Me rotates about the C–N bond such that its Me group moves away from the Me group on the pyrimidinone ring of an adjacent molecule. Thus, it is the Me···Me repulsion and not the C–H···O/halogen attraction that determines the conformation in this crystal structure. Although the conformation of the *N*-tolyl moiety is different from the Br–Ph, I–Ph and NO_2–Ph groups, the 2D polar layer arrangement is a recurring pattern in all these structures. The details of crystal packing in **1***m*-Me are different from that in the **1***m*-Br and **1***m*-I structures, notwithstanding that methyl-halogen mimicry[25] is a common phenomenon in crystal structures. If the methyl and halogen structures are different, as in this case, it is usually a result of specific, directional interactions controlling the crystal packing and not mere space filling of hydrophobic groups. We believe that the weak C–H···halogen interaction and Me···Me repulsion are responsible for differences in crystal packing between Me and halogen analogues. It has been possible to probe the role of such subtle effects in crystal packing because a series of molecules with minor substituent variations were synthesised, and their crystal packing analysed systematically.

In **1***m*-OMe (space group $C2/c$), translation-related molecules are connected *via* the C–H···O chain synthon (2.45 Å, 161°) and the OMe group is involved in forming (Ph)C–H···O dimers between inversion-related molecules (2.70 Å,

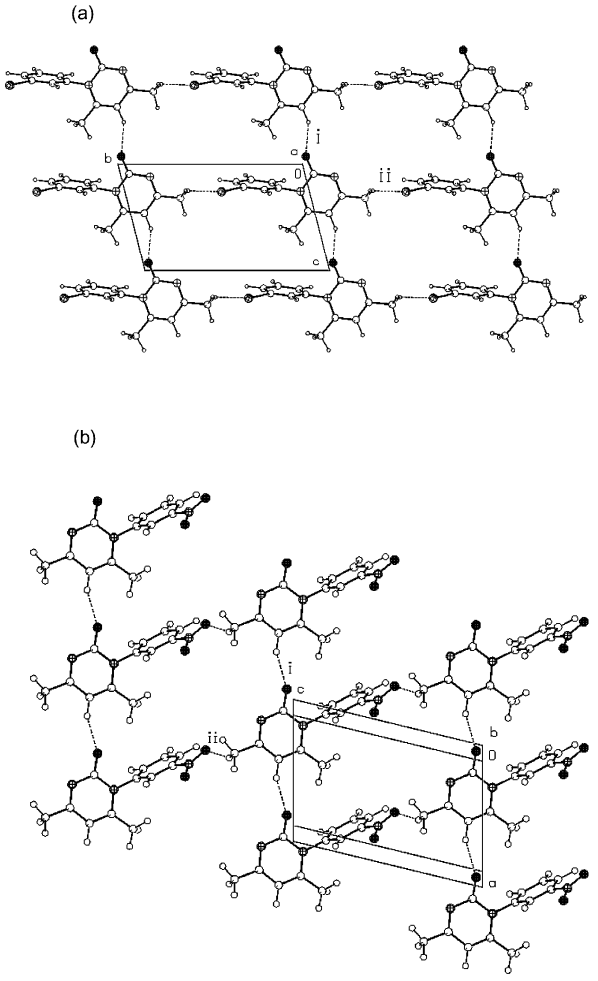

Fig. 3 (a) 2D polar layer arrangement in **1***m*-I mediated by C–H···O and C–H···I interactions i and ii. (b) 2D polar layer of **1***m*-NO_2. Note the similarity in the 2D networks.

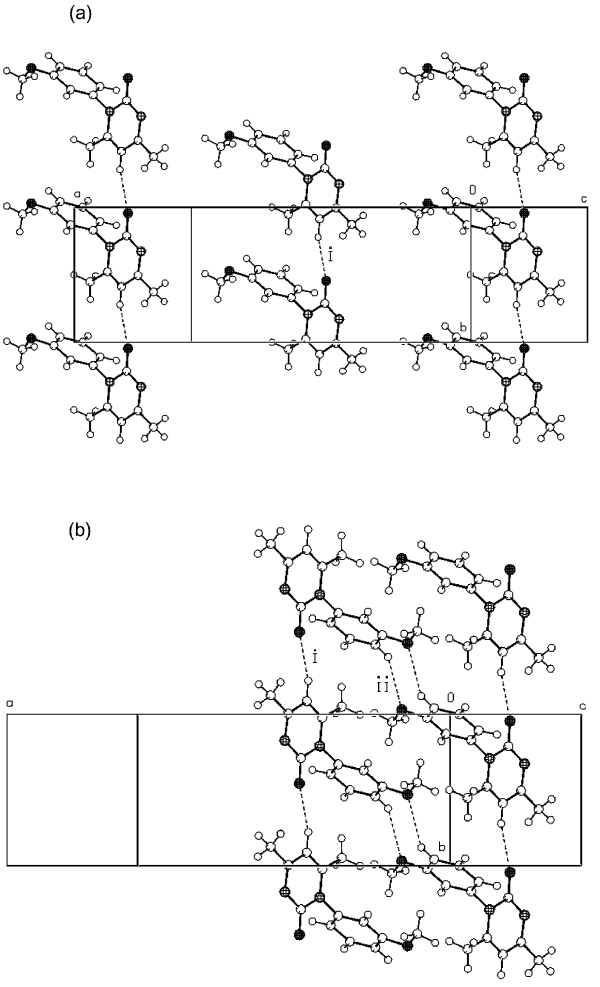

Fig. 5 (a) 2D polar layer in **1***m*-OMe with 1D chains oriented in the same direction. (b) Centrosymmetric C–H···O interactions between anisyl rings of inversion-related molecules.

137°; Fig. 5). All this suggests that the C–H···O chain supramolecular synthon is an invariant structural motif in the 2D polar layer pattern. Other weak hydrogen bonds in the lateral direction, such as C–H···O and C–H···halogen, determine the overall 3D structure. There is thus a hierarchy of interactions even within the weak hydrogen bond category: the 1D chain and the 2D layer interactions are predictable, but the factors that control the stacking of layers are difficult to dissect.

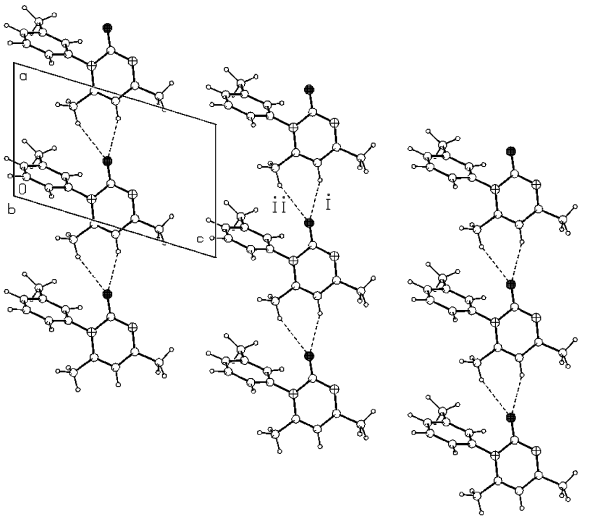

Fig. 4 2D polar layer in **1***m*-Me. The conformation of the *m*-tolyl ring is different compared to the orientation of the phenyl ring in Figs. 2 and 3.

1,2-Dihydro-*N*-*meta*-fluorophenyl-4,6-dimethylpyrimidin-2-one

Crystallisation of **1***m*-F from benzene–ethyl acetate afforded diffraction quality single crystals that solved and refined in the space group *Pnma*. The *meta*-fluoro derivative shows structural features that serve as a bridge between the unsymmetrical *meta* compounds and the symmetrical *para* series. Although the molecule has an unsymmetrical phenyl substitution, the crystal system has a mirror plane *m*, similar to the unsubstituted and *para* compounds (**1**H, **1***p*-Me, **1***p*-Cl).[13a] The pyrimidinone molecule resides in the mirror plane and this plane bisects the *N*-*m*-fluorophenyl ring ([Fig. 6(a)]. This structure is isostructural with **1***p*-Me, **1***p*-Cl (*Pnma*) in that the 1D chains are oriented parallel within the 2D polar layer. However, it is different from the structure of **1**H (*Pbcm*) in which 1D chains are aligned anti-parallel in the layer. Normally, replacement of H with F in a molecule does not result in significant structural differences[26] because the van der Waals radius of these atoms is similar (H_{vdW} 1.20, F_{vdW} 1.47 Å). However, when the H and F structures are different, specific C–H···F interactions may be involved. Analysis of the inter-layer packing in **1***m*-F shows that there is a (Me)C–H···F interaction [2.59 Å, 125°; Fig. 6(b)] between inversion-related molecules. The F atom is refined with a site-occupancy of 0.5; the pyrimidinone ring

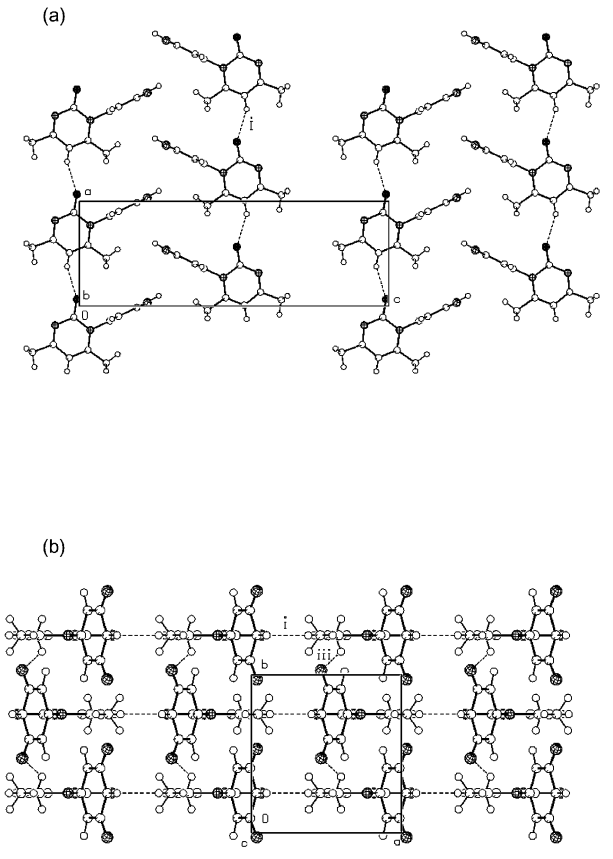

Fig. 6 Crystal structure of **1***m*-F. (a) Parallel alignment of 1D chains sustained by C–H···O interaction i. (b) Interlayer C–H···F interaction iii. The F atom has 0.5 occupancy in each location. The space group and arrangement of molecules is identical to the **1***p*-Me and **1***p*-Cl structures.[13a]

atoms reside in the mirror plane and are fully ordered. A possible reason for the 50% occupancy of fluorine could be that in this way the unsymmetrical phenyl ring conforms to the higher mirror symmetry in the crystal. This suggests that the presence of mirror plane *m* in the crystal is an important steering factor. This may be traced to the pyrimidinone molecule having the stable bisected-phenyl conformation.[13] Normally, molecules do not reside on the *m* special position because this arrangement decreases packing efficiency by 2–3%.[24,27] However, retention of *m* or 2 symmetry is thermodynamically advantageous because the molecules are symmetrically arranged. All in all, a number of factors such as molecular symmetry, energy of the conformation in the crystal, and weak intermolecular interactions (C–H···O, C–H···halogen) determine the final packing motif in the crystal structure. Regarding the nature of fluorine disorder in the crystal, that is, whether it is static or dynamic,[28] this issue can be answered only with variable low-temperature X-ray diffraction studies. The present X-ray data were collected at about ambient temperature.

1,2-Dihydro-*N*-methyl-4-methyl-6-phenylpyrimidin-2-one and 1,2-dihydro-*N*-methyl-4-phenyl-6-methylpyrimidin-2-one

The unsymmetrical molecules, 4-Me-6-Ph analogue **2a** and 4-Ph-6-Me analogue **2b**, were synthesised to extend conjugation of the phenyl ring with the pyrimidinone heterocycle to enhance the molecular hyperpolarisability. Since the structures of these two isomers could not be unambiguously ascertained by NMR spectroscopy (see Experimental), the final assignment was made after X-ray diffraction. The structures shown as **2a** and **2b** were confirmed from the ORTEP plots [Fig. 7(a,b)]. In **2a** (*Pbca*), the molecules are organised in a zigzag array *via* C–H···O hydrogen bonds that extend into corrugated sheets Fig. 7(c)]. The *N*-Me group is disordered. In **2b** (*C*2/*c*), the linear C–H···O chain is preserved [Fig. 7(d)]. The hydrogen-bonded layers are 2D polar in both crystal structures, suggesting that the parallel alignment of 1D chains in a 2D layer motif is a characteristic feature of the pyrimidinone family. To summarise, variation in the position of alkyl and aryl residues on the molecular skeleton does not disturb the main C–H···O hydrogen bond synthon and the 2D polar layer organisation in these crystal structures.

The main idea behind synthesising molecules **2** was to extend the conjugated chromophore as compared to pyrimidinone **1**. While 2D polarity is routinely achieved, the absence of 3D non-centrosymmetry in these crystals makes further attempts to optimise the molecular hyperpolarisibility for inducing SHG effects somewhat of a futuristic goal. The task of controlling the parallel alignment of 1D dipoles or 2D polar layers in non-centrosymmetric space groups (*e.g.*, $P2_1$, *Fdd*2, $Pna2_1$, *Imm*2), namely crystals that lack an inversion centre, is still a difficult challenge with no general solution to the problem. In a recent review, Lin[8b] has discussed this issue in terms of the number of interpenetrating 3D networks and proposed that odd-fold catenation is likely to result in non-centrosymmetric crystal packing.

Model for 2D polar layers

The occurrence of 2D polar layers is a repeating theme in the pyrimidinone family of crystal structures. The changes in substitution range from simple exchange of groups on the *N*-aryl moiety to the replacement of phenyl with methyl groups on the pyrimidinone ring. While the space groups and detailed packing motifs vary from crystal to crystal, the 1D chain of C–H···O hydrogen bonds and the 2D polar layer assembly are invariant structural features. This prompted us to understand the phenomenon of 2D polarity in terms of the molecular structure of **1** and the robust C–H···O hydrogen bond synthon in these crystals. Our model is based on the fact that molecules of **1** form a linear array of C–H···O hydrogen bonds. Such chains may then align either in a parallel fashion (2D polarity) or in an anti-parallel arrangement (a common layer motif). Four possible arrangements of hydrogen-bonded chains of molecules **1** in a 2D layer are displayed in Fig. 8. Motifs a and b are 2D polar while the chains are aligned anti-parallel in c and d. The most common pattern in pyrimidinone crystals is depicted in motif a. Translation-related molecules form the C–H···O hydrogen-bonded chain (in the direction of the arrow) and such chains are in turn connected through weak hydrogen bonds or van der Waals interactions involving the phenyl ring. This 2D polar motif is present in eight structures, three from previous studies (**1**H·HCl, **1***p*-Me·HCl, **1***p*-Cl·HCl)[13] and five in this paper (**1***m*-Br, **1***m*-I, **1***m*-NO_2, **1***m*-Me, **1***m*-OMe). In motif b, a two-fold screw axis or a glide plane parallel to the polar (arrow) direction relates molecules in adjacent chains. This results in the stable herringbone geometry between phenyl rings and the methyl groups close-pack on the other side. The 2D polar motif b is present in four structures (**1***p*-Me, **1***p*-Cl, **1***p*-Ph and **1***m*-F). In the anti-parallel arrangement c, the interactions are similar to those in a but the symmetry operation that relates the hydrogen-bonded molecules is different. A 2_1-screw axis or a glide plane perpendicular to the polar (arrow) direction relates adjacent chains that run in opposite directions within a layer. Only three structures (**1**H, **1***p*-Me·HNO_3, **1***p*-Cl·HNO_3) belong to this category. Motif c is not preferred, despite having similar interactions and void size compared to motif a, because the methyl group in **1** is not correctly placed within the molecule to have a lateral interaction with a substituent on the phenyl group (dotted lines), as depicted in motif c. A hydrogen bond between the phenyl ring and pyrimidinone heterocycle in the

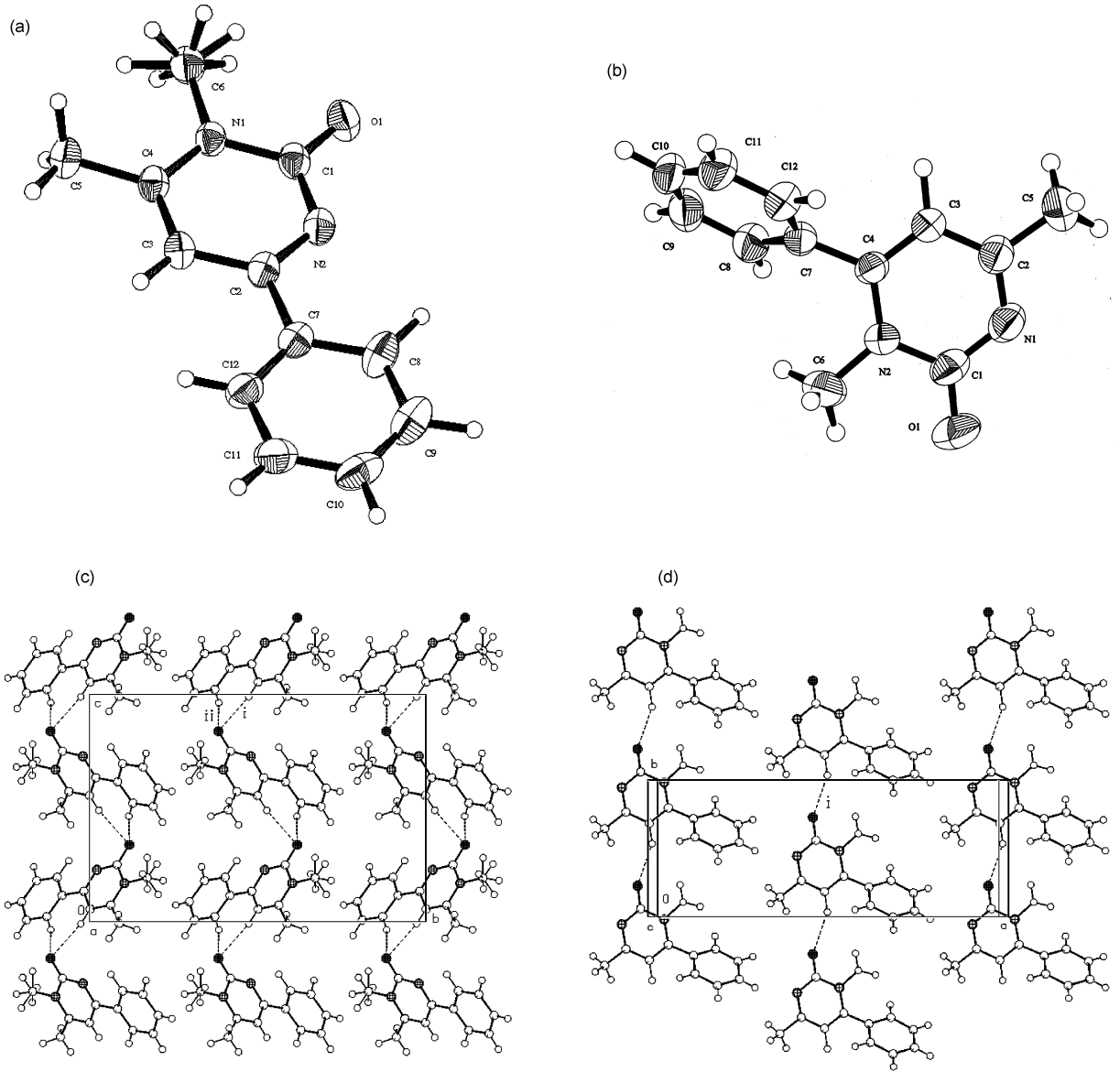

Fig. 7 ORTEP plot of *N*-methyl-4-methyl-6-phenylpyrimidinone **2a** (a) and *N*-methyl-4-phenyl-6-methylpyrimidinone **2b** (b). The N–Me group in **2a** is disordered. (c) 2D polar corrugated layer in **2a**. (d) 2D polar layer assembly in **2b**. Note the recurrence of a parallel alignment of dipolar molecules within a layer in **1** and **2**.

lateral direction would be bent in arrangement c. The centrosymmetric layer (motif d), with adjacent chains related by an inversion centre, is not observed in any structure. This is because inversion symmetry is not compatible with the ubiquitous herringbone T-geometry between phenyl rings in the solid state.[29] Even though inversion-related phenyl rings can engage in π-π stacking, this motif may not be favoured in the present case because quadrupole-quadrupole interactions (charge-transfer component) between like phenyl rings may be minimal. Thus, the dominant 2D polar layer arrangement is rationalised through motifs a and b that account for 12 of the 15 crystal structures studied. The proposed model is specific to the molecular structure of *N*-aryl pyrimidinone **1**. A better understanding of the factors that promote 2D polarity in these structures will emerge from an analysis of more diverse and complex systems.

Conclusions

A study of the factors that promote crystallisation of 1D chains or 2D layers of molecules in polar space groups is a current theme in crystal engineering, with implications in materials science. It has been shown in recent papers that non-centrosymmetric crystal packing may be achieved with 1D chains sustained by C–H···N interactions[30] and in 2D layers connected *via* C–H···O interactions.[31] The parallel alignment of dipoles in these crystal structures is explained through weak hydrogen bonds.‡

Two-dimensional layered structures assembled with O–H···O and N–H···O hydrogen bonds in crystals of uronium salts, imidazole carboxylates and urea derivatives have been reported.[15,16] We have shown in this paper the recurrence of 2D polar networks in *N*-aryl pyrimidinone crystals, thereby emphasising that robust and reliable C–H···O synthons offer an equally effective crystal design theme[32] as the strong hydrogen bonds. The role of steric and/or electronic effects in hydrogen bonding and crystal packing has been examined by the systematic variation of functional groups in a family

‡ Non-linear dielectric property in hydrogen-bonded chains may be established with strong O–H···O, N–H···O (KH_2PO_4, urea) or weak C–H···O, C–H···N bonds (ref. 30, 31). The issue here is not whether the interaction is strong or weak but has more to do with the perfect polar alignment of chromophores in the crystal.

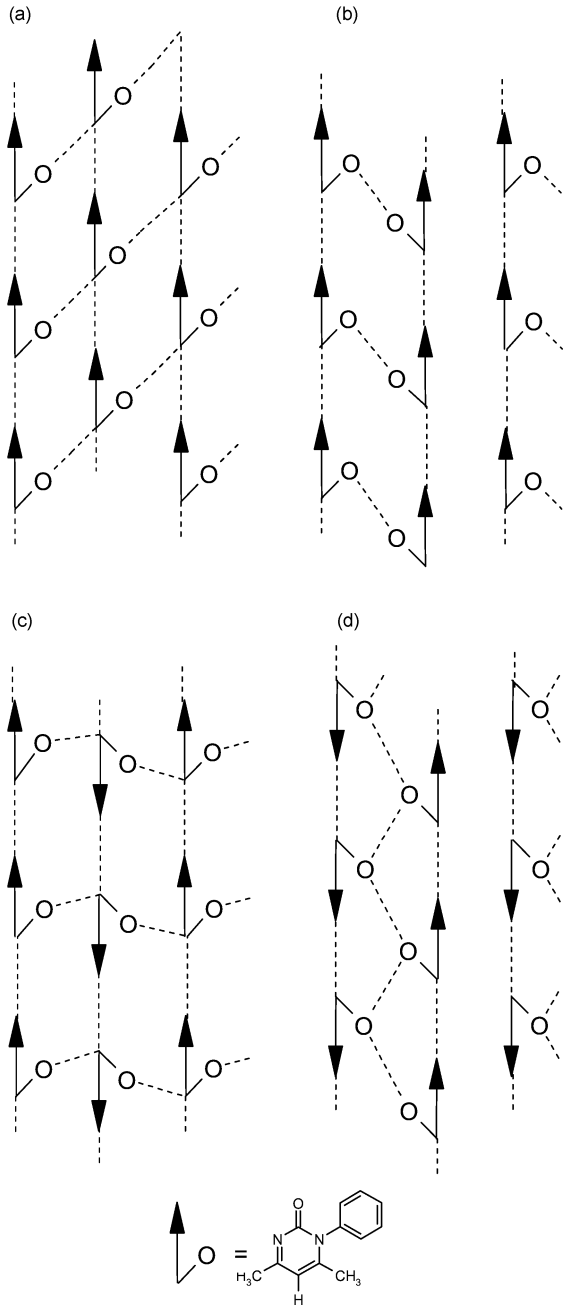

Fig. 8 Model to explain the recurrence of the 2D polar layer arrangement in phenyl pyrimidinone **1**. The 1D chain is constructed with C–H···O interactions in all cases while the lateral interactions in the layer are different. (a) Parallel alignment of 1D chains and lateral C–H···X interactions are simultaneously optimised. (b) Parallel alignment of 1D chains and herringbone motif between phenyl groups. (c) Anti-parallel alignment of 1D chains, the lateral C–H···X interaction is bent. (d) Anti-parallel alignment of 1D chains with neighbouring phenyl groups being inversion-related. Motif a is present in over half the structures studied (8/15), motif b in 4 and motif c in 3 structures. Motif d is not found in any structure. See text for details.

of structures. The present study shows that a combination of molecular features and hydrogen bond synthons direct the self-assembly of 2D polar layers. The parallel stacking of such layers into non-centrosymmetric 3D crystals is a continuing challenge in our ongoing studies.

Acknowledgements

We thank the Indo-French Centre for the Promotion of Advanced Research for financial support (Project 1708-1).

References

1 (*a*) J.-M. Lehn, *Supramolecular Chemistry*, VCH, Weinheim, 1995; (*b*) *Perspectives in Supramolecular Chemistry. The Crystal as a Supramolecular Entity*, ed. G. R. Desiraju, Wiley, Chichester, 1995, vol. 2.
2 G. R. Desiraju, *Crystal Engineering. The Design of Organic Solids*, Elsevier, Amsterdam, 1989.
3 J. W. Steed and J. L. Atwood, *Supramolecular Chemistry*, Wiley, Chichester, 2000.
4 R. D. Rogers and M. J. Zaworotko, *Trans. Am. Crystallogr. Assoc.*, 1998, **33**, 1.
5 G. R. Desiraju and T. Steiner, *The Weak Hydrogen Bond in Structural Chemistry and Biology*, Oxford University Press, Oxford, 1999.
6 (*a*) F. H. Allen and W. D. S. Motherwell, *Acta Crystallogr., Sect. B*, 2002, **58**, 407; (*b*) A. Nangia, *CrystEngComm*, 2002, **4**, 93.
7 G. R. Desiraju, *Angew. Chem., Int. Ed. Engl.*, 1995, **34**, 2311.
8 (*a*) B. Moulton and M. J. Zaworotko, *Chem. Rev.*, 2001, **101**, 1629; (*b*) O. R. Evans and W. Lin, *Acc. Chem. Res.*, 2002, **35**, 511.
9 J. Hulliger, H. Bebie, S. Kluge and A. Quintel, *Chem. Mater.*, 2002, **14**, 1523.
10 (*a*) M. D. Hollingsworth, *Curr. Opin. Solid State Mater. Sci.*, 1996, **1**, 514; (*b*) P. J. Langley and J. Hulliger, *Chem. Soc. Rev.*, 1999, **28**, 279.
11 (*a*) K. T. Holman, A. M. Pivovar and M. D. Ward, *Science*, 2001, **294**, 1907; (*b*) K. T. Holman, A. M. Pivovar, J. M. Swift and M. D. Ward, *Acc. Chem. Res.*, 2001, **34**, 107.
12 O. R. Evans, R. G. Xiong, Z. Y. Wang, G. K. Wong and W. B. Lin, *Angew. Chem., Int. Ed.*, 1999, **38**, 536.
13 (*a*) M. Muthuraman, Y. L. Fur, M. Bagieu-Beucher, R. Masse, J.-F. Nicoud, S. George, A. Nangia and G. R. Desiraju, *J. Solid State Chem.*, 2000, **152**, 221; (*b*) S. George, A. Nangia, M. Muthuraman, M. Bagieu-Beucher, R. Masse and J.-F. Nicoud, *New. J. Chem.*, 2001, **25**, 1520.
14 J. Zyss and J.-F. Nicoud, *Curr. Opin. Solid State Mater. Sci.*, 1996, **1**, 533.
15 For recent studies, see: (*a*) V. Videnova-Adrabinska and E. Janéczko, *J. Mater. Chem.*, 2000, **10**, 555; (*b*) J. C. MacDonald, P. C. Dorrestein and M. M. Pilley, *Cryst. Growth Des.*, 2001, **1**, 29.
16 (*a*) Y.-L. Chang, M.-A. West, F. W. Fowler and J. W. Lauher, *J. Am. Chem. Soc.*, 1993, **115**, 5991; (*b*) L. M. Toledo, J. W. Lauher and F. W. Fowler, *Chem. Mater.*, 1994, **6**, 1222; (*c*) B. Gong, C. Zheng, E. Skrzypczak-Jankun, Y. Yan and J. Zhang, *J. Am. Chem. Soc.*, 1998, **120**, 11 194.
17 (*a*) S. Brasselet, F. Cherioux, P. Audebert and J. Zyss, *Chem. Mater.*, 1999, **11**, 1915; (*b*) W. Lin, Z. Wang and L. Ma, *J. Am. Chem. Soc.*, 1999, **121**, 11 249; (*c*) C. Bourgogne, Y. L. Fur, P. Juen, P. Masson, J.-F. Nicoud and R. Masse, *Chem. Mater.*, 2000, **12**, 1025; (*d*) C. C. Evans, R. Masse, J.-F. Nicoud and M. Bagieu-Beucher, *J. Mater. Chem.*, 2000, **10**, 1419.
18 (*a*) C. C. Evans, M. Bagieu-Beucher, R. Masse and J.-F. Nicoud, *Chem. Mater.*, 1998, **10**, 847; (*b*) M. Muthuraman, R. Masse, J.-F. Nicoud and G. R. Desiraju, *Chem. Mater.*, 2001, **13**, 1473.
19 R. Thaimattam, C. V. K. Sharma, A. Clearfield and G. R. Desiraju, *Cryst. Growth Des.*, 2001, **1**, 103.
20 T. Hertzsch, S. Kluge, E. Weber, F. Budde and J. Hulliger, *Adv. Mater.*, 2001, **13**, 1864.
21 *Vogel's Textbook of Practical Organic Chemistry*, revised by B. S. Furniss, A. J. Hannaford, P. W. G. Smith and A. R. Tatchell, ELBS Longman, Essex, 5th edn., 1989, pp. 964–966.
22 (*a*) A. Altomare, M. Cascarano, C. Giacovazzo and A. J. Guagliardi, *J. Appl. Crysallogr.*, 1993, **26**, 343; (*b*) teXsan for Windows, v. 1.03, Single Crystal Structure Analysis Software, version 1.04, Molecular Structure Corp., Woodlands, TX , USA, 1997–98; http://www.msc.com; (*c*) *International Tables for Crystallography*, ed. A. J. C. Wilson, Kluwer Academic, Dordrecht, 1992, vol. C, Table 4268, pp. 6111–2; (*d*) A. L. Spek, Platon97, Bijvoet Centre for Biomolecular Research, University of Utrecht, The Netherlands.
23 (*a*) P. K. Thallapally and A. Nangia, *CrystEngComm.*, 2001, 27; (*b*) L. Brammer, E. A. Bruton and P. Sherwood, *Cryst. Growth Des.*, 2001, **1**, 277; (*c*) F. Neve and A. Crispini, *Cryst. Growth Des.*, 2001, **1**, 387.
24 A. I. Kitaigorodsky, *Molecular Crystals and Molecules*, Academic Press, New York, 1973.
25 M. R. Edwards, W. Jones, W. D. S. Motherwell and G. P. Shields, *Mol. Cryst. Liq. Cryst.*, 2001, **356**, 337.
26 A. Nangia, *New J. Chem.*, 2000, **24**, 1049.

27 C. P. Brock and J. D. Dunitz, *Chem. Mater.*, 1994, **6**, 1118.
28 R. Boese, M. Y. Antipin, D. Bläser and K. A. Lyssenko, *J. Phys. Chem. B*, 1998, **102**, 8654.
29 (*a*) C. Janiak, *J. Chem. Soc., Dalton Trans.*, 2000, 3885; (*b*) W. B. Jennings, B. M. Farrell and J. F. Malone, *Acc. Chem. Res.*, 2001, **34**, 885.
30 M. Ohkita, T. Suzuki, K. Nakatani and T. Tsuji, *Chem. Commun.*, 2001, 1454.
31 P. K. Thallapally, G. R. Desiraju, M. Bagieu-Beucher, R. Masse, C. Bourgogne and J.-F. Nicoud, *Chem. Commun.*, 2002, 1052.
32 C. K. Broder, M. G. Davidson, V. T. Forsyth, J. A. K. Howard, S. Lamb and S. A. Mason, *Cryst. Growth Des.*, 2002, **2**, 163.